ARTICLES

Single Molecule Study of Perylene Orange Photobleaching in Thin Sol−Gel Films

C. Julien, A. Débarre,* D. Nutarelli, A. Richard, and P. Tchénio

Laboratoire Aimé Cotton, UPR CNRS 3321, Bâtiment 505, Campus d'Orsay, 91405 Orsay Cedex, France

Received: May 9, 2005; In Final Form: September 20, 2005

The paper reports on photobleaching mechanisms of perylene orange embedded in thin sol−gel films, derived from single molecule studies. The experimental configuration uses wide-field illumination and one photon excitation of the molecules. Measurements have been performed both at ambient conditions and under vacuum in order to get information on the influence of oxygen on photobleaching in such porous samples. We have also recorded the evolution of photobleaching with respect to the excitation intensity. The results demonstrate that photobleaching from excited states higher than the first singlet and triplet states has a nonnegligible contribution as soon as the excitation energy exceeds a few hundred W/cm^2 and that this process is favored in the presence of air. The study also demonstrates that perylene orange in sol−gel films is not a very efficient emitter but that photobleaching can be slow, which explains the interest for perylene orange as a good candidate to produce long lifetime solid-state lasers when embedded in monoliths of sol−gel.

Introduction

Sol−gel matrixes offer the opportunity of easily trapping guest molecules inside their porous framework. Moreover, sol−gel material is processed at low temperature, which prevents photodegradation of the doping molecules. Additionally, sol−gel properties can be modified by the large choice of precursors available. Different devices such as solid-state laser media, electrooptics, or sensors exploit these properties. In the latter case, the sensitivity relies on the ability of a doping molecule trapped in a pore to interact with a molecule diffusing through the porous matrix. The efficiency of such systems depends on the aging properties of the doped sol−gel. Among them, photobleaching is a limiting process since it cancels the activity of the doping molecule. Two main mechanisms have been proposed to explain photobleaching, photochemical oxidation of the molecule on one hand and multiphoton ionization on the other hand. The relative weight of the two processes largely depends on the properties of the local surroundings of the molecule, on the molecule itself, and on external parameters such as excitation power.

In the present work, the system of interest is a thin sol−gel film, doped with perylene orange molecules. This molecule was synthesized at the end of the 1980s.[1] Studies have been performed in order to quantify its ability for efficient lasing in the visible, either in solution or incorporated in solid matrixes including sol−gels.[2−8] Processed as films, sol−gels can be used as coatings or as nanometric sensors. To derive information on film properties, we have performed single molecule studies that give access to the fluctuations of the fluorescence from one molecule to the other, a very revealing method.[9−12] As the emission properties of a molecule are deeply connected to its interaction with its local environment, Single molecule spectroscopy (SMS) offers in fact the opportunity of probing the heterogeneity of a sample. A lot of studies have been performed on average properties of sol−gel films or monoliths[13−19] and to address the physicochemical properties of sol−gel samples at the nanoscale.[20−25]

In this paper, we focus on photobleaching. SMS allows us to probe the distribution of molecule photobleaching behaviors. Such a knowledge is of main interest since the applications of thin sol−gel films will indeed crucially depend on the photostability of the dopants. Perylene orange molecules were observed by wide-field microscopy either at ambient conditions or under vacuum and at different excitation intensities. One interest of wide-field imaging is to follow the fluorescence of several hundred of molecules in parallel, under identical conditions. By recording stacks of images of the same sample area versus time, one accesses the dynamics of the emission. After the Experimental Section, we first qualitatively discuss the results obtained on two pertinent data per molecule, the so-called survival time and the total number of emitted photons before bleaching occurs. We then tentatively derive more quantitative information on the bleaching mechanisms from a simple five electronic level model. In the discussion, we show that, despite the limits of this model, we can retrieve information on the kinetic behaviors of perylene encapsulated in sol−gel films, which were quite unexpected. These results will also be discussed in the light of recent studies on the photobleaching kinetics of rhodamine 6G in solution and in poly(vynyl alcohol) (PVA).[26−28]

Experimental Section

Sample Preparation. Perylene orange, also named KF241 or BASF241, has been chosen because of its photostability, as well as its large emission spectral range, as already checked in thick solid sol−gel matrixes.[6−8] Its chemical structure is displayed in Chart 1. This nonpolar, nonionic molecule is not

* Corresponding author: anne.debarre@lac.u-psud.fr.

10.1021/jp052398x CCC: $30.25
Published on Web 11/17/2005

CHART 1: Chemical Structure of Perylene Orange

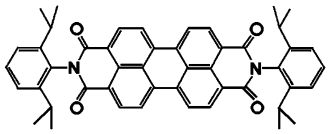

soluble in water but in nonpolar solvents. To reach a satisfying dispersion of the molecules into the sample, the precursor is MTEOS (methyltriethoxysilane) and the sol−gel is of ormosil type. The acid hydrolysis of MTEOS is performed in an equimolar ethanol−water solution mixture. Hydrolysis solvents are then removed and replaced by a weakly doped perylene orange THF (tetrahydrofuran) solution. The final concentration of dopants in the sol is 10^{-11} M. The sol is allowed to age in the dark and then spin-coated on clean cover glasses at 8000 rpm. Film thickness varies between 50 and 100 nm. The concentration in the sol has been empirically adjusted in order to attain a satisfying dispersion of the molecules after spin casting at a speed needed to get thin films. The thinness of the film was controlled by atomic force microscopy measurements, and the concentration was chosen so that the mean distance between adajcent molecules was of the order of a few micrometers.

Single Molecule Imaging. Fluorescence images are acquired with a wide-field microscope. Light from an argon ion laser at 514 nm is coupled into the entry of a single-mode fiber, which acts as a point source. The size and the divergence of the beam are controlled by a system of two achromatic lenses. In the wide-field configuration, the beam slightly diverges at the back entrance of the objective. A pinhole selects a more homogeneous part of the beam before the back pupil, and a narrow-band excitation filter is added in the incoming path. The beam is then reflected into the objective by a dichroic mirror at 514 nm. The typical illuminated area of the sample is of the order of 2000 μm^2 by using a 40× NA 1.3 oil immersion objective. Intensity varies from 75 to 7000 W/cm^2. The Airy spot diameter is 480 nm. Fluorescence of the molecules is backward collected by the same objective and sent to a CCD camera (CoolSnap, Photometrics) through the $f = 160$ mm tube lens. An Alpha Epsilon edge filter (Omega AELP 520) eliminates the residual laser light in the detection path. The total detection efficiency is estimated to be 10%. Contrary to confocal microscopy, wide-field illumination does not involve spatial filtering in the image plane and the signal-to-background ratio greatly depends on the optimization of the acquisition time and of sample properties. In the present situation, thinness and transparency of the sample efficiently reduce the background signal. A satisfying compromise is obtained for acquisition times ranging from a few tenths to some seconds depending on the excitation intensity. Nevertheless, residual diffusion at 514 nm needs to be suppressed in order to unambiguously identify the locations of molecules and then analyze their signal. The sample is held in a chamber connected to a fluidic system, which allows us to work under an inert atmosphere or under a vacuum of about 10^{-4} mbar. At the initial concentration of 10^{-11} M in the sol before aging and spin casting, about 200 emitters are excited in the active area. The large number of emitters observed despite the low initial concentration indicates a rather efficient evaporation of the volatile solvent (THF) during the elaboration of the samples. To perform an analysis on this large number of molecules, we developed dedicated software that first treats the images in order to eliminate the diffusion background. Then the gravity center of each fluorescent spot is automatically determined. Fluorescence intensity is then obtained for every single molecule for each image, which allows us to derive the temporal traces of the molecules in a given film. This software exploits the particular properties of the emission of single molecules, especially those related to size and shape of the molecule image spot determined by the spatial resolution and the magnification of the microscope. The semiautomatic analysis is interactive, and the user can verify or even eliminate some questionable data. It offers the opportunity to work with large enough molecular sampling to derive a representative statistical analysis of the molecular behavior.

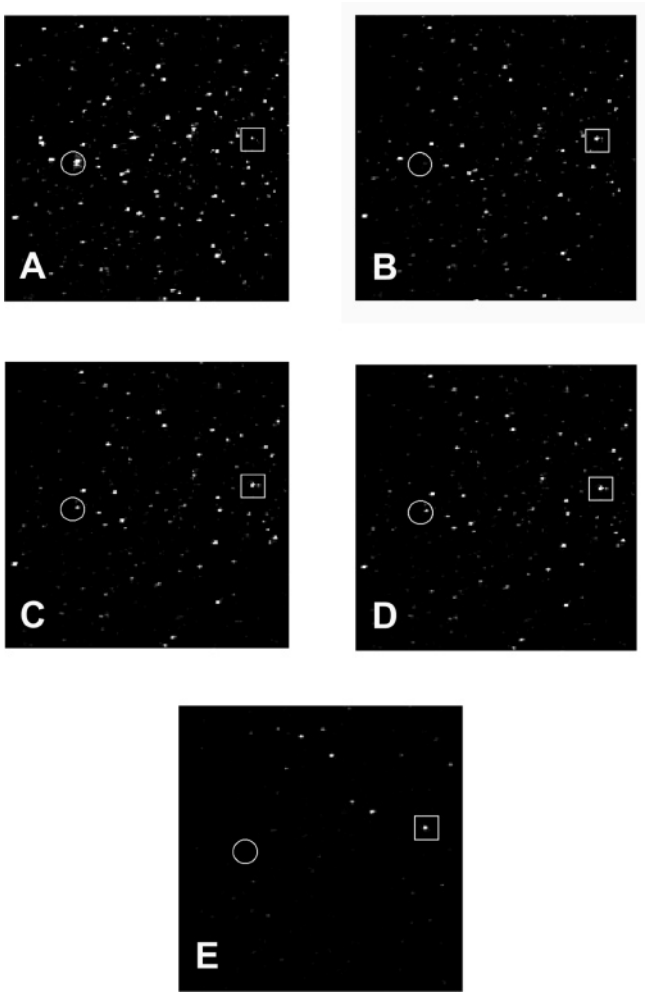

Figure 1. Sequence of five treated images of a film recorded under vacuum at an excitation intensity of 1400 W/cm^2. The two framed molecules illustrate the case of a molecule of long survival time (square) and the blinking process (circle). From upper row to lowest and from left to right, images were acquired after 700 ms, 1.4 s, 3.5 s, 4.2 s, and 415 s, respectively, size 890 μm^2.

Results

An example of five treated images of a film, acquired under vacuum, is given in Figure 1, to point out typical behaviors of single perylene orange molecules. Each image is acquired in 700 ms with an excitation energy of 1400 W/cm^2. The first remark concerns the broad distribution of intensities of the molecules. Some spots are very bright while others are dim. To be sure that every spot corresponds to a single molecule and not to a small cluster or to an impurity, we have systematically made polarization controls at different steps of the film acquisition. A thin Wollaston prism is inserted into the detection path, which allows us to compare the relative intensities of two-orthogonal polarizations of the fluorescence

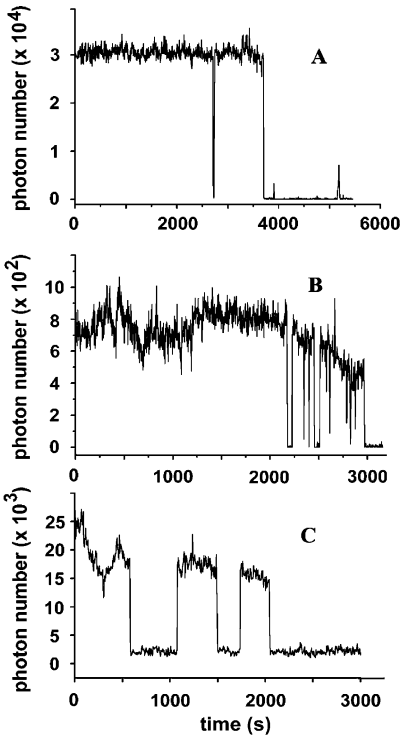

Figure 2. Examples of kinetics traces: (A) under vacuum, excitation intensity 75 W/cm^2; (B) at ambient conditions, excitation intensity 75 W/cm^2; (C) same conditions as A. B and C cases are illustrations of the different time scales of the blinking process observed in thin sol−gel films.

emission under a linearly polarized excitation. For most of the bright objects, the two components are not equal, which indicates that the objet is polarized and eliminates the possibility that it could be a cluster. In other cases, the two components are nearly equal. It can be a cluster of molecules, despite the low concentration of dopants. But this situation can also be encountered at least in two cases for a single molecule. First, it can correspond to a single molecule, whose dipole is directed perpendicularly to the sample or at 45° of the linear polarization of the incident beam. Second, it can correspond to a molecule that freely tumbles inside a pore as already observed by Viteri et al.[24] An additional test is therefore necessary to determine the nature of the object.

One possibility is to analyze the fluorescence kinetics trace. Three examples are displayed on Figure 2. The first example corresponds to the classical behavior expected for a fixed molecule. The intensity is fairly constant until it drops definitively to zero in a single step because of photobleaching. This time corresponds to the survival time τ of the molecule. The long lasting emission is only interrupted once by a blinking process. The second example is also a classical situation encountered in single molecule spectroscopy. The emission level oscillates between the background value and a constant upper level. This well-known behavior corresponds to blinking, here to be distinguished from photon antibunching that occurs at a smaller time scale. In the actual trace, blinking starts after a long period of emission stability, which might result from a slight diffusion of the molecule toward a location where quenching is favored. It could also result from the diffusion of an O_2 molecule in the neighboring of the perylene orange molecule.[29] The third example corresponds to a situation for which the rate of blinking is slow and the molecule undergoes a transition between two states nearly equally probable, one emissive and the other dark.

Intensity distribution partly reflects the distribution of dipole orientations with respect to laser polarization, but depolarization alone cannot explain the variety of kinetic behaviors of the emitters. In fact while some spots last for very long times under irradiation (several hours at low-intensity irradiation), many others disappear very rapidly and some disappear several times for a while then reappear. These features first reflect the broad heterogeneity of the sol−gel film, as already reported.[13,21,22,30] In fact, the different sites in which the molecules are trapped are not equivalent. For example, fluorescence can be partly quenched if it sits near a wall, depending on the polarity of the pore. The kinetics trace distribution also reflects the hetereogeneity of the properties of the sol−gel film with respect to photobleaching. In particular, emission can be very stable in a limited number of sites, much more stable than should be the emission of the molecules directly deposited on glass for example.[31] The sol−gel matrix partly protects the dopants against rapid photobleaching, and it explains the efforts devoted to design devices based on doped sol−gels.

In fact, one main interest of single molecule studies is to provide two independent parameters for each doping molecule: the total number of photons emitted by each molecule before photobleaching N_t and the survival time τ. We have derived histograms of N_t, for the different recorded films as well as the relevant histograms of τ (Figures 3 and 4). To get more insight into this process, films were acquired at ambient conditions and under vacuum for intensities in the range 75−6500 W/cm^2. The acquisition time for a given film depends on the excitation intensity and varies typically from 500 ms/image at highest intensities up to 3 s/image for the lowest ones. The determination of the survival times is only accurate for molecules that last several images, whereas the N_t value is still accurate for these molecules. In fact, even for the largest value, the excitation intensity is not very high and few molecules among the statistical sample die within the first image or two. The relevant error in the first peak value of the histograms is therefore negligible.

First characteristics of the involved processes can be derived from a qualitative comparison of histograms from air to vacuum at 75 W/cm^2 (Figure 5). Let us focus first on the histogram of N_t. Under both environments, most of the molecules emit less than 2.5×10^6 photons, which is somewhat surprising with respect to the claimed high quantum efficiency of perylene orange.[1,3] N_t reaches 1.2×10^8 for the strongest emitter under vacuum and 1 order of magnitude less in air. If only 10% of molecules emit more than 10^7 photons under vacuum, it drops to 2% in air. This rate remained low regardless of the excitation power. The typical expected fluorescence rate of an efficient dye near saturation is of the order of some 10^7-10^8 photons/s. At the highest used excitation energy $I \simeq I_S/2.5$, under vacuum, the highest rates measured for single molecules are in the range of a few 10^5 photons/s, far from this value.

Whereas a comparison of the results with previous experiments is always questionable because they are quite sensitive to the system itself and to experimental conditions (especially to excitation energy), it might be useful to replace the results in a more general context. A typical value of 10^4 photons/s was reported for Rh 6G doped into poly(methylacrylate), under vacuum, at intensities of about 10^4 W/cm^2, higher than our largest value.[32] More closely related to the present work is the average rate of 2.5×10^3 photons/s measured at an excitation energy of 350 W/cm^2 for a single peryleneimide dendrimer (g0) dispersed in poly(vinylbutyral).[33] Correspondingly, most of the molecules survive less than roughly 15 min either under vacuum or in air, but some special individuals last several hours, up to

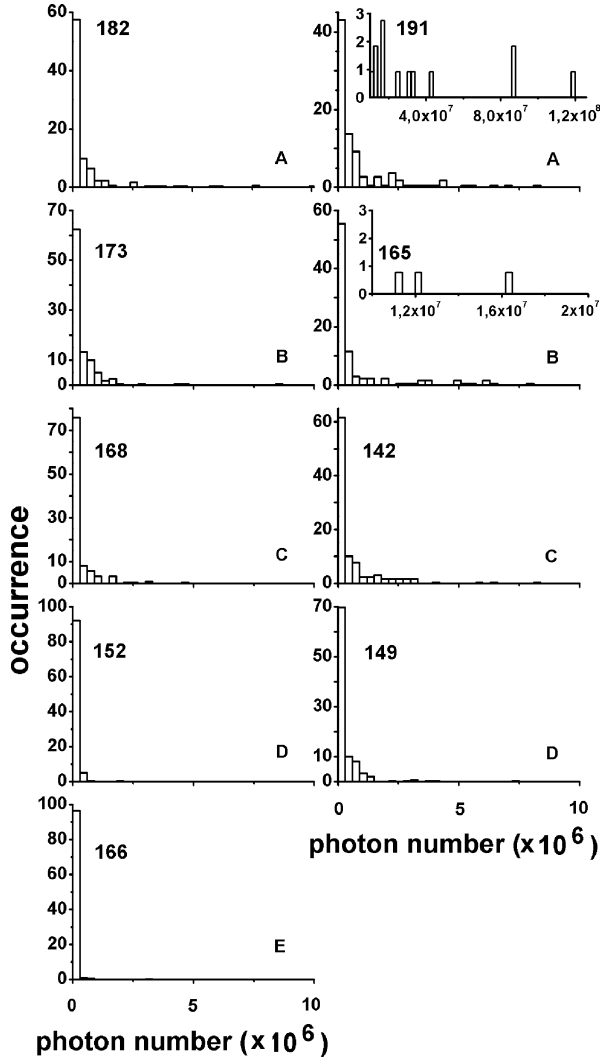

Figure 3. Histograms of the percentage of molecules emitting a given number of photons for increasing intensity from top to bottom, in air on left side and under vacuum on right side: (left side) 75 (A), 200 (B), 750 (C), 2015 (D), 6450 W/cm^2 (E); (right side) 75 (A), 375 (B), 755 (C), 1410 W/cm^2 (D). In insets, tails of the histograms.

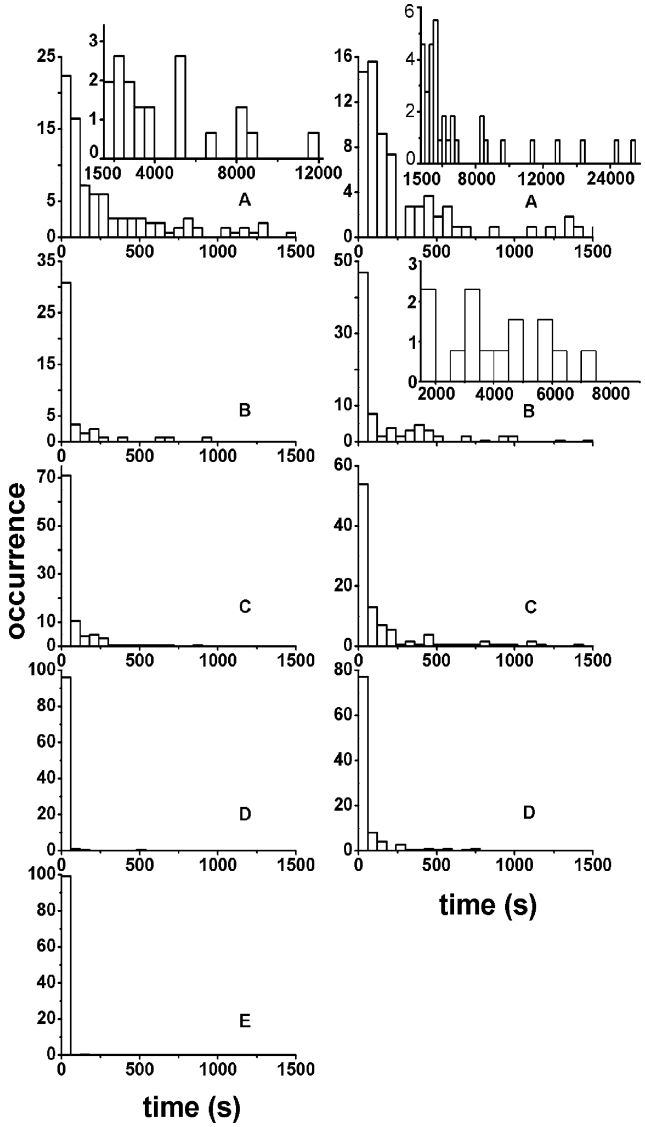

Figure 4. Histograms of the percentage of molecules as a function of their survival time τ. Same samples and same disposition and symbols as in Figure 3.

nearly 7 h under vacuum and up to 3 h in air. There is no systematic correlation between strong emission and long survival time, and the emission rate is most often moderate. There is in fact a broad dispersion of the on intensity level. The highest emission rate under vacuum, nearly 10^5 photons/s, corresponds to a molecule that emits 2×10^7 photons before dying. Low emission rates of a few 10^3 photons/s are also observed for molecules that survive only during some images. More generally, photon rates range from 2×10^2 to 10^5 photons/s, and these values show that perylene orange in sol−gel films is not a very efficient emitter. The broad distribution of photon rates is in line with a large heterogeneity of the sample and random orientation of the probes. All these observations have an equivalent in air, even though the emission rate distribution is sligthly expanded toward the low values. It ranges from 1.2×10^4 photons/s to a few tens of photons/s for molecules that disappear very rapidly. The emission rate distribution as well as its absolute values are nevertheless comparable in air and under vacuum. In particular a rough comparison between levels in air and under vacuum indicates that these levels are of the same order of magnitude and that their distribution is nearly similar.

In air, one identified bleaching process is the collision of the molecule with an oxygen singlet.[34−38] This process implies a first step corresponding to the formation of a complex between O_2 and the molecule in its triplet state, leading to singlet oxygen formation during the quenching of the triplet state of the excited molecule.[39] This latter process results in an increased cycling efficiency of the molecule, if photobleaching does not occur. Consequently, one could expect to observe a general trend of increase of the level of intensity in air with respect to vacuum, which is not the case. At least two possibilities can explain this observation. First, if an O_2 molecule collides with the molecule in its triplet state, the probability of subsequent photodegradation is high, because of the confinement in the complex porous structure. Second, the level of emission might not be solely governed by the properties of the triplet state, as suggested below by further results.

In a homogeneous sample, the histograms of the number of fluorescence photons emitted by the molecules as well as those of their survival times can be fit by a single-exponential decay.[40,41] Whatever the conditions—air or vacuum—it is not the case for our histograms. Berglund et al. have recently underlined the importance of the uniformity of the excitation profile in the analysis of the fluorescence decay.[42] In fact, an inhomogeneous profile should cause a multiexponential decay, even in a homogeneous sample. We have tried, as far as

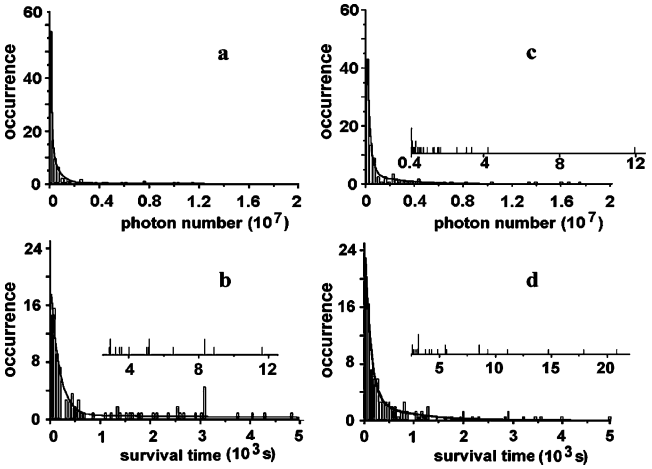

Figure 5. Fit of the histograms of N_t and τ at 75 W/cm^2 in air (left) and under vacuum (right). The fitting function is $A \exp(-x/\alpha) + B \exp(-x/\beta)$ in both cases. Parameters of the fit: (a) $\alpha = 8.4 \times 10^4$, $\beta = 6 \times 10^5$; (b) $\alpha = 105$ s, $\beta = 800$ s; (c) $\alpha = 2.5 \times 10^5$, $\beta = 2.7 \times 10^6$; (d) $\alpha = 180$ s, $\beta = 7000$ s. In insets, tails of the histograms.

possible, to limit this bias. First, a pinhole located ahead of the objective selects nearly $^2/_3$ of the full width at half-maximum of the laser spot. Second, only a reduced part of the image is retained for the quantitative analysis, which ensures that as a whole the intensity fluctuations are less than at most 20%. As a result, the non-monoexponential decay mostly reflects the heterogeneity of sol−gel media. As displayed in Figure 5, even two exponential decays are not sufficient to fit the histograms in detail. In fact, it does not account for the longest survival or strongest emissive molecules. It however demonstrates that at least two subpopulations exist in the sample, in agreement with the observations of Viteri et al.,[24] which show that both the histograms of the tumbling molecules and of the fixed molecules can be fitted by a two-exponential decay. As expected, the shortest exponential decay time of 180 s is longer under vacuum. However, it is only a factor of about 2 larger than that obtained in air. As this average survival time is related to the bleaching rate, the limited difference between the two values indicates that photooxidation is probably not the only photobleaching process or that it also plays a role under vacuum despite the low pressure. In both cases, about 43% of molecules survive less than this characteristic time. Histograms of N_t follow the same general characteristics (Figure 5). Let us turn to the evolution of the histograms with respect to excitation intensity. As displayed on Figures 3 and 4, the most striking point is that this evolution is not similar under vacuum and in air. In both cases, the number of molecules of short survival times increases with increasing intensity, but the rate is much faster under air. For example at 754 W/cm^2 under vacuum there are still many emitters that last more than 10^3 s, whereas at 200 W/cm^2 in air, only one emitter lasts 2200 s. A similar conclusion can be derived from the analysis of the histograms of the number of photons. More precisely, if we focus on the evolution of the histogram of the total number of photons in air, we observe a clear tightening with increasing power. Such a tightening is not expected for single photon bleaching processes. First, it indicates that photobleaching under ambient conditions does not occur solely from the first excited states of the molecules. Second it implies that the relevant higher order processes have a contribution of the same order of magnitude than the single-photon ones, which was not a priori expected in air. The latter conclusion also applies under vacuum, which is less unexpected since photooxidation from the first triplet state should be reduced. Unfortunately, these results cannot be directly compared to other

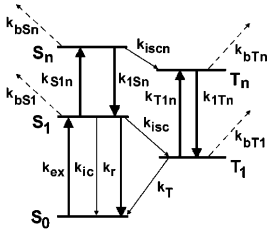

Figure 6. Schematics of the dynamics of the molecule based on an electronic five-level system. All parameters are detailed in the text.

SMS results either on perylene orange itself or on a related peryleneimide. In fact, to our knowledge, SMS studies have only been conducted on more complex systems, namely, rigid dendrimers with a well-defined number of peryleneimide chromophores.[33,43,44] Nevertheless, our observations are in line with the general result that whatever the analyzed parameter, survival time, or emissivity, large fluctuations are observed in conjunction with the heterogeneity of the matrix.

Quantitative Analysis

To derive more quantitative information on the specific photobleaching processes for perylene orange embedded in sol−gel films, we consider in this paragraph the average values $\bar{N}_t$ and $\bar{\tau}$ of the total numbers of fluorescence photons and survival times, respectively, as a function of the excitation intensity I (W/cm^2), assumed to be constant on the illuminated area. The experimental results have confirmed that the sample is heterogeneous as expected, but the idea that sustains the analysis of the average values is that the statistics are sufficient to derive effective rate constants of the dominant bleaching processes. More precisely, the number of analyzed molecules is around 200 molecules for any given film.

The qualitative conclusions of the previous paragraph imply that it is necessary to consider at least a five electronic level system to describe the molecular system. The classical relevant diagram is displayed on Figure 6. The five levels are the ground state S_0, the first and higher excited singlet states S_1 and S_n, and the two first and higher triplet states T_1 and T_n. k_r, k_{ic}, k_{isc}, k_T, k_{Sn1}, and k_{Tn1} are the radiative and nonradiative decay rates from S_1 to S_0, the nonradiative intersystem crossing rate from S_1 to T_1, the decay rate from T_1, and the radiative decay rates from S_n and T_n to S_1 and T_1, respectively. k_{01}, k_{S1n}, and k_{T1n} are the excitation rates from S_0 to S_1, S_1 to S_n, and T_1 to T_n, respectively. The latter are proportional to the relevant absorption cross section σ_{ij} at the given wavelength λ and to the excitation intensity, $k_{ij} = \sigma_{ij} I(hc/\lambda)$, where c is light velocity.

Population rate equations can be written as

$$\frac{dS_0}{dt} = -k_{01}S_0 + (k_r + k_{ic})\,S_1 + k_T T_1$$

$$\frac{dS_1}{dt} = k_{01}S_0 + k_{S_{n1}}S_n - (k_r + k_{ic} + k_{isc} + k_{S_{1n}})S_1 - k_{bS_1}S_1$$

$$\frac{dT_1}{dt} = k_{isc}S_1 + k_{T_{n1}}T_n - (k_T + k_{T_{1n}})\,T_1 - k_{bT_1}T_1$$

$$\frac{dS_n}{dt} = k_{S_{1n}}S_1 - (k_{S_{n1}} + k_{bS_n})S_n$$

$$\frac{dT_n}{dt} = k_{T_{1n}}T_1 - (k_{T_n1} + k_{bT_n})T_n \qquad (1)$$

k_{bS_i}, k_{bT_i} stand for the photobleaching rates from the states S_i ($i = 1, n$) and T_i ($i = 1, n$), respectively. The intersystem crossing

rate from the higher level S_n has been neglected with respect to the short lifetime of the upper levels, of the order of a few hundreds of femtoseconds. The rates of photobleaching are expected to be small compared to the other rates and population probabilities can be derived from the steady-state regime of a closed system for which $S_0 + S_1 + T_1 + S_n + T_n = 1$. Equilibrium population probabilities can be written as

$$S_0^{eq} = \frac{k_{T_{n1}} k_{S_{n1}} k_T k_f}{k_{T_{n1}} k_T [k_{S_{n1}}(k_f + k_{01}) + k_{01} k_{S_{1n}}] + (k_{T_{n1}} + k_{T_{1n}})(k_{isc} k_{S_{n1}} k_{01})}$$

$$S_1^{eq} = \frac{k_{01}}{k_f} S_0^{eq}$$

$$T_1^{eq} = \frac{k_{isc}}{k_T} S_1^{eq}$$

$$S_n^{eq} = \frac{k_{S_{1n}}}{k_{S_{n1}}} S_1^{eq}$$

$$T_n^{eq} = \frac{k_{T_{1n}}}{k_{T_{n1}}} T_1^{eq} \quad (2)$$

where $k_f = k_r + k_{ci} + k_{isc}$.

In our experiments, the highest excitation intensity is lower than 10^4 W/cm^2, and pumping rates toward S_n and T_n can be neglected in a first analysis in the expression of S_1^{eq}. As a result S_1^{eq} reduces to its expression for a three-level system

$$S_1^{eq} = \frac{k_{01} k_T}{k_f k_T + k_{01}(k_T + k_{isc})} = \frac{I/I_S}{1 + I/I_S}\left(\frac{k_T}{k_T + k_{isc}}\right) \quad (3)$$

and

$$I_S = \frac{k_f k_T}{\sigma_{01}\frac{\lambda}{hc}(k_T + k_{isc})}$$

I_S is the saturation intensity. The total effective photobleaching rate can be written as

$$k_B^T = (k_B^{1h\nu} + k_B^{2h\nu} I)\, S_1^{eq} \quad (4)$$

with

$$k_B^{1h\nu} = k_{bS_1} + k_{bT_1}\frac{k_{isc}}{k_T}$$

$$k_B^{2h\nu} = \frac{\lambda}{hc}\left(\frac{k_{bS_n}}{k_{S_{n1}}}\sigma_{S_{1n}} + \frac{k_{bT_n}}{k_{T_{n1}}}\frac{k_{isc}}{k_T}\sigma_{T_{1n}}\right)$$

where $k_B^{1h\nu}$ and $k_B^{2h\nu}$ are the total rates of the photobleaching processes following one- and two-photon absorption, respectively. We use a very simple model in order to derive the expression of $\bar{N}_t$, assuming that photobleaching results from a quasi-unimolecular reaction, which is reasonable with respect to the entrapment of the molecules in the matrix. In this model, we neglect the heterogeneity of the environments of the molecules, which means that we are interested in determining whether the average behavior can be described by a single effective bleaching parameter k_B^T, as defined by eq 4.

$$\bar{N}_t = \int_0^{t\to\infty} k_r S_1^{eq} \exp(-k_B^T t)\, dt = k_r \frac{1}{k_B^{1h\nu} + k_B^{2h\nu} I} \quad (5)$$

The second pertinent parameter $\bar{\tau}$ inversely corresponds to the effective photobleaching rate k_B^T. It can be written as

$$(\bar{\tau})^{-1} = \left(\frac{I/I_S}{1 + I/I_S}\right)\left(\frac{k_T k_B^{1h\nu}}{k_T + k_{isc}}\right)\left(1 + \frac{k_B^{2h\nu}}{k_B^{1h\nu}} I\right) \quad (6)$$

These two parameters can be compared to the values deduced from the measurements at different excitation powers. Figure 7 displays the experimental data for $\bar{N}_t$ and $(\bar{\tau})^{-1}$ in air and under vacuum. Solid curves represent the relevant fits deduced from eqs 5 and 6 and parameter values are grouped in Table 1, assuming that the lifetime of the first singlet excited level is 3 ns, which is a typical value for that type of dye.

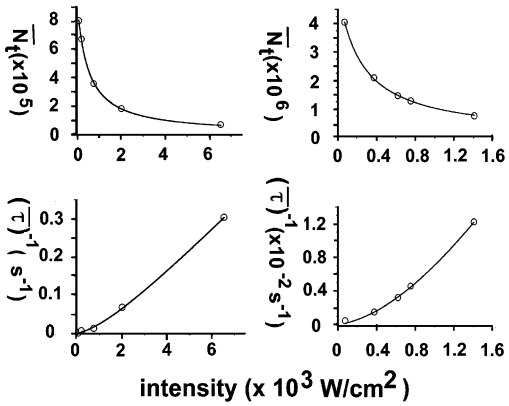

Figure 7. Experimental data (circles) and fits (full lines) of the average number of emitted photons $\bar{N}_t$ and of the inverse of the average survival time $(\bar{\tau})^{-1}$ with respect to the excitation intensity, in air (left) and under vacuum (right). For a model of the fits, see text; for parameters, see Table 1.

TABLE 1: Average Photophysical Parameters[a]

	vacuum	air
$k_B^{1h\nu}$ (s^{-1})	56 ± 6	322 ± 49
$k_B^{2h\nu}$ (s^{-1}·W^{-1}·cm^2)	0.24 ± 0.04	0.66 ± 0.10
I_S (W·cm^{-2})	$3.8 \times 10^3 \pm 1.1 \times 10^3$	$2.6 \times 10^3 \pm 0.4 \times 10^3$
$k_T/(k_T + k_{isc})$	$1.2 \times 10^{-4} \pm 0.4 \times 10^{-4}$	$0.9 \times 10^{-4} \pm 0.2 \times 10^{-4}$

[a] See text for the definition of the parameters.

Discussion

If we focus on the single-photon photobleaching rate, it is clear that the relevant one-step process is nearly six times more efficient in air than under vacuum, as expected if the photobleaching mechanism involves collisions with singlet oxygen from the first triplet state. More surprisingly, under any condition, air or vacuum, a two-photon process occurs with a nonnegligible probability as soon as the excitation intensity exceeds a few hundreds of W/cm^2. At about 500 W/cm^2 for air and 250 W/cm^2 for vacuum this process reaches the same rate as that of the single-photon process. Furthermore, this process is more efficient in air than under vacuum, which was not expected. It is in line with the observation of a rapid histogram shrinkage in air with increasing intensities. These results point out the importance of two-photon photobleaching as soon as excitation intensity exceeds a moderate value in a sol−gel film. The single photon photobleaching rate, measured in air in the sol−gel film, is of the same order of magnitude as the values

obtained for rhodamine 6G in water, deduced from cell experiments, and between the values derived from fluorescence correlation spectroscopy for dyes such as Rh6G or TMR in water.[45] It indicates that perylene orange is probably quite a reactive dye. The marked difference between the values in air and under vacuum proves that the sol−gel film is highly porous and that reactive species such as oxygen or water play a role in the single photon photobleaching process, as expected. Competition between single and two-photon photobleaching starts at moderate intensities (around 100 W/cm^2), in a range of intensities between the values measured for Rh6G dispersed in PMA[32] and in water.[45] In the case of the PMA sample, which is maintained under vacuum, the two-photon process is dominant even at very low irradiances. In the case of the solution of Rh6G, the two-photon process is observed for irradiances above about 10^4 W/cm^2. This difference can be explained by the fact that the dye is diluted in a solvent in which dissolved oxygen can be present, but it may also result from the protic character of water, which favors charge-transfer processes, another possible mechanism for photobleaching. Furthermore, owing to nonnegligible probability of collisions between the dye molecules in a liquid, the lifetime of the first excited states decreases with respect to a situation where the molecules are trapped, as in PMA or sol−gel samples. Our results confirm that photobleaching is highly dependent on the environment of the molecules and on the chemical nature of the molecule itself. The rate constant of the single photon photobleaching for the sol−gel film under vacuum is lower than that in air but still not negligible, whereas the external oxygen flow is reduced by more than 7 orders of magnitude at working pressures around 10^{-4} mbar. However, some pools can entrap residual water produced by hydrolysis despite the pumping procedure used during the elaboration process. If they are relatively deeply located, pumping during observation results in a slow vapor flow across the sample, which could partly explain the residual value of the single photon photobleaching. Another possibility relies on a different mechanism of single-photon photobleaching for which oxygen is not involved, as explained above. When the molecule is excited, part of its energy can be converted into rotation or into translation and the molecule can slowly diffuse to a location of appropriate chemical nature where quenching is favored. If polar groups such as silanols partly cover the molecule environment, hydrogen bonding followed by quenching can occur and the molecule stops emitting.

Photobleaching processes depend not only on the environment of the molecule but also on its chemical nature. Bird et al. have calculated that the energy of the first triplet state of two perylene derivatives, named, DBPI (bis((2,5-di-*tert*-butylphenyl)imide)) and DXP (bis((2,6-dimethylphenyl)imide)), is about half the energy of higher excited triplet states, which favors a two-photon excitation toward T_n.[46] Perylene orange has, in fact, a structure that differs from that of DXP molecule only by the substituants on the pending phenyl rings, which suggests that a two-photon excitation process could also be rather efficient in our system, opening the path to two-photon photobleaching.

Beyond the efficiency of the two-photon process, another striking observation is the higher rate value obtained in air. It suggests in turn that the reaction could be assisted by a species present under these conditions and able to pick up the electron released by the molecule in a photoionization reaction. This could be the case of molecular oxygen, leading to the formation of $O_2^{\cdot -}$. This observation can also be connected to the existence of a transient ionic state in the presence of a radical, as suggested by Zondervan et al. in their study on rhodamine 6G doped in PVA.[27,28] If the probability of creating a radical ion in an oxidizable site of the matrix cannot be discarded, it is much lower than for rhodamine 6G. Despite the nonionic character of peryleneimides (PI), the existence of such a radical has been evoked in the work of Vosch et al. on rigid dendrimers including PI.[44] This possibility is suggested in order to explain one of the off processes in the millisecond range, observed in the temporal fluorescence traces of a single molecule. Indeed, if an ionic state of lower energy than the first triplet is created and stabilized by interaction with oxygen or with the walls of the sol−gel pores, a new channel of photobleaching appears involving one-photon ionization to higher ionic states. This hypothesis could explain a higher rate of two-photon photobleaching in air than under vacuum.

The saturation values I_s, deduced from the fit of the inverse of the average survival time, are of same order of magnitude as those observed for molecules of peryphenethyl dispersed in thin sol−gel films, under vacuum[47] or for Rh6G molecules dispersed in PMA also under vacuum.[32] On the contrary, the values deduced for the parameter $k_T/(k_T + k_{isc})$ are surprisingly low, on the order of 10^{-4}. On another hand, another value of this ratio can be deduced from the fitted value of I_s (eq 3). Assuming a typical absorption cross section of 10^{-16} cm^2, $k_T/(k_T + k_{isc})$ takes a value of 0.33×10^{-2} and 0.23×10^{-2} under vacuum and air, respectively. The discrepancy between the two values of the ratio cannot be explained by the experimental and fit uncertainties (Table 1). Consequently, it implies that a five electronic level system is not sufficient to accurately describe the kinetics of perylene orange in thin sol−gel films.

Let us give some arguments sustaining this conclusion and discuss them with respect to related works. A low value of the ratio $k_T/(k_T + k_{isc})$ implies that $k_{isc} \gg k_T$. This condition can be fulfilled if the triplet lifetime of perylene orange is very long, on the order of hundreds of milliseconds. It would then depart from some other peryleneimides for which triplet lifetime was measured. For peryphenethyl indeed, triplet lifetime deduced from autocorrelation measurements was of the order of 150 μs.[47] The same order of magnitude has been obtained for perylene-imide (PI) attached to dendrimers in deoygenated diethyl eher.[48] Precise measurements of triplet lifetimes of PI in similar rigid dendrimers doped into PMMA or zeonex at normal atmospheric conditions or under nitrogen atmospheric conditions reveal that the triplet lifetime of PI does not exceed 1.5 ms, using either continuous or pulsed excitation.[44] Very long triplet lifetime is thus unlikely. Furthermore, we can note that a low k_t rate should be rather contradictory with the observation that a nonnegligible number of emitters have very long survival times, since photobleaching efficiency should increase with triplet lifetime in air. A second possibility is that the intersystem crossing rate reaches very large values, not in line with the values observed in the dendrimers that do not exceed 4.8×10^3 s^{-1}. Both assumptions (a long triplet lifetime or a large value of k_{isc}) underlie that the molecule would spend on average much more time in the dark triplet state than on the excited S_1 state. If this was correct, it would imply that such a situation would be induced by the coupling between the molecule and the sol−gel, otherwise perylene orange should be an inefficient dye even in solution. Results suggest the presence of a long-lived nonemissive state, different from S_0 and T_1, which should be stabilized by the interaction of the molecule and the sol−gel matrix.

One interesting remark is that such an unexpected low value of the ratio $k_T/(k_T + k_{isc})$ is also observed in a study of the photobleaching dynamics of rhodamine 6G in PVA.[27,28] In these

studies, the authors deduce from their measurements the values of the two parameters k_T and k_{isc}. If the latter has a value close to what is expected, the former is very weak of the order of 10 s^{-1} at low intensity. To explain this anomalous weak value, the authors suggest that in their sample a long-lived state is created by the stabilization of a radical ion. The energy of this transient ionic state is lower than that of the first triplet state. In fact, the well-known ionic character of rhodamine 6G supports this hypothesis.

The introduction of an additional ionic state of energy lower than the triplet one is equivalent to consider an effective triplet state in the five electronic level system leading to different kinetics parameters for population, deexcitation, and photobleaching. This remark is corroborated by the thorough analysis of the photobleaching kinetics of rhodamine 6G of Eggeling et al. in water,[26] which gives very useful insights into the different kinetics of the dye under continuous, picosecond, or subpicosecond excitation. The authors show that under continuous illumination, photobleaching of rhodamine 6G in a particulary oxidant solvent (water) can be correctly described by a simple five model system. In our system, the presence of such an ionic state could account for the increased two-photon photobleaching in air. Nevertheless, it should lead to the observation of weak saturation values, which is not the case. In conclusion, taking into account such a low energy level is not sufficient to explain the observations in our case.

Let us turn to another possibility, related to the structure of the molecule. The particular dynamics of perylene orange in sol−gel films could be induced by a change of conformation of the molecule. This reconformation could take place in the excitation state S_1. Such a dynamic is at the origin of dual emission that has been much studied since its first observations on bianthryl, for example.[49] When this situation occurs, photophysical parameters as k_{isc} can undergo large changes. For perylene orange, this reconformation could imply a reorientation of the ending phenyl groups that make a nearly 90° angle with the perylene core in the ground state. This type of reconformation has been observed for example by Rettig et al. in the case of a biphenyl substituted molecule, the 4-(*N*,*N*-dimethylamino)-4′-cyanobiphenyl.[50] However, the compatibility between low values of $k_T/(k_T + k_{isc})$ and values of I_s in the range of a few kW/cm^2 implies that this reconformed state should decay very rapidly. This assumption is not in agreement with values reported in the literature especially as regards the decay time of a CT state. Another convincing possibility corresponds to the occurrence of a reconformation of the molecule in the ground state, leading to the existence of at least one conformer with a low absorption. The molecule in such a trapping state no longer cycles until the conformation relaxes to S_0, but its survival time increases since it is protected against photobleaching when in the "dark sate". In this case, the fluorescence efficiency of the molecule depends on the equilibrium kinetics between the conformers. This latter assumption is in line with the observation that a nonnegligible fraction of molecules has long survival times, whereas their fluorescence rate is quite low. It can also explain the kinetics of traces frequently observed, for which dark periods as long as several tens or hundreds of seconds separate emissive ones. Furthermore, it is in agreement with the fact that perylene orange trapped in sol−gels could be used as long lifetime solid-state dye lasers.[7] In fact, in the trap state, molecules act as a pool for further lasing.

Conclusion

Wide-field single molecule microscopy was used to study the bleaching behavior of perylene orange molecules entrapped in thin sol−gel films. One of the main results concern the surprisingly high efficiency of bleaching from highest S_n and T_n states reached by two-photon excitation with respect to photobleaching from S_1 and T_1 states. This process is efficient for excitation intensities far below the saturation intensity. A second important result is that a two-photon photobleaching process is more efficient in air than under vacuum, which can be explained if the photoionization is assisted by a molecule present under ambient conditions. Beyond the statistical microscopic analysis, we have performed an analysis of the average behavior of the molecular kinetics, based on a classical five-level model. If this model allowed us to retrieve some main characteristics of the observation, especially as concerns the two-photon bleaching process, it fails to explain the rather low rates of fluorescence measured, not in line with the assumed efficiency of this dye. It suggests the possibility of an additional unidentified dark state, different from the first triplet level, likely to be a conformer with low absorption. As a result, a five-level system is not sufficient to thoroughly explain the kinetics of the molecules embedded in a thin sol−gel film. On another hand, a severe approximation underlies the use of such quantitative simple models in heterogeneous samples. We have assumed that the statistics of molecules was sufficient to erase the fluctuations of the behaviors of the molecules with respect to their local environment. In other words, the above simple model applies for a homogeneous sample, or at least for a given identified homogeneous subpopulation of molecules. Nevertheless, the dispersion of the fluorescence rate values is not too high and heterogeneity alone is not likely to explain the discrepancy between the five-level model and the measurements. To progress in the understanding of the kinetics of perylene orange in such films, the next step is to record the timing of the fluorescence photon emission to retrieve photophysical parameters among which the lifetime of the triplet state T_1 as well as to analyze fluorescence spectra at the level of single molecules, to determine a possible change of conformation of the molecule in the film. Work is in progress on the latter point.

Acknowledgment. We thank Drs. J.-P. Boilot and F. Chaput (Laboratoire de la Matière Condensée, UMR 7643 CNRS, Ecole Polytechnique, 91128 Palaiseau cedex, France) for providing the thin sol-gel films.

References and Notes

(1) Seybold, G.; Wagonblast, G. *Dyes Pigm.* **1989**, *11*, 303.
(2) Ivri, J.; Burshtein, Z.; Miron, E.; Reisfeld, R.; Eyal, M. *IEEE J. Quantum Electron.* **1990**, *26*, 1516.
(3) Reisfeld, R.; Seybold, G. *Chimia* **1990**, *44*, 295.
(4) Canva, M.; Georges, P.; Perlgritz, J.-F.; Brun, A.; Chaput F.; Boilot J.-P. *Appl. Opt.* **1995**, *34*, 428.
(5) Rahn, M. D.; King, T. A. *Appl. Opt.* **1995**, *34*, 8260.
(6) Rahn, M. D.; King, T. A.; Gorman, A. A.; Hamblett, I. *Appl. Opt.* **1997**, *36*, 5862.
(7) Qian, G.; Yang, Y.; Wang, Z.; Yang, C.; Yang, Z.; Wang, M. *Chem. Phys. Lett.* **2003**, *368*, 555.
(8) Faloss, M.; Canva, M.; Georges, P.; Brun, A.; Chaput, F.; Boilot, J.-P. *Appl. Opt.* **1997**, *36*, 6760.
(9) Tamarat, Ph.; Maali, A.; Lounis, B.; Orrit, M. *J. Phys. Chem. A* **2000**, *104*, 1 and references therein.
(10) Eggeling, C.; Widengren, J.; Rigler, R.; Seidel, C. A. M. In *Applied Fluorescence in Chemistry, Biology and Medicine*; Rettig, W., Strehmel, B., Schrader, S., Siefert, H., Eds.; Springer-Verlag: Berlin, 1999; pp 193−239.
(11) Yip, W.-T.; Hu, D.; Yu, J.; Vanden Bout, D. A.; Barbara, P. F. *J. Phys. Chem. A* **1998**, *102*, 7564.
(12) Dickson, R.-M.; Cubitt, A. B.; Tsien, R. Y.; Moerner, W. E. *Nature* **1997**, *388*, 355.
(13) Keeling-Tucker, T.; Brennan, J. D. *Chem. Mater.* **2001**, *13*, 3331.
(14) Avnir, D.; Levy, D.; Reisfeld, R. *J. Phys. Chem.* **1984**, *88*, 5956.

(15) Dunn, B.; Zink J. I. *Chem. Mater.* **1997**, *9*, 2280.
(16) Dunn, B.; Zink J. *J. Mater. Chem.* **1991**, *1*, 903.
(17) Panday, S: Baker, G. A.; Kane, M. A.; Bonagni, N. J.; Bright, F. V. *Chem. Mater.* **2000**, *12*, 3547.
(18) Casalboni M.; De Matteis, F.; Ferone, V.; Prosposito, P.; Senesi, R.; Pizzoferrato, R.; Bianco, A.; De Mico, A. *Chem. Phys. Lett.* **1998**, *291*, 167.
(19) Suratwala, T.; Gardlund, Z.; Davidson, K.; Ulhmann, D. R.; Watson, J.; Peyghambarian, N. *Chem. Mater.* **1998**, *10*, 190.
(20) Hou, Y.; Bardo, A. M.; Martinez, C.; Higgins D. A. *J. Phys. Chem. B* **2000**, *104*, 212.
(21) Mei, E.; Bardo, A. M.; Collinson, M. M.; Higgins D. A. *J. Phys. Chem. B* **2000**, *104*, 9973.
(22) Bardo, A. M.; Collinson, M. M.; Higgins, D. A. *Chem. Mater.* **2001**, *13*, 2713.
(23) Higgins, D. A.; Collinson, M. M.; Ginagunta, S.; Bardo, A. M. *Chem. Mater.* **2002**, *147*, 3734.
(24) Viteri, C. R.; Gilliland, J. W.; Yip, W. T. *J. Am. Chem. Soc.* **2003**, *125*, 1980.
(25) Baumann, R.; Ferrante, C.; Kneuper, E.; Deeg, F.-W.; Br äuchle C. *J. Phys. Chem. A* **2003**, *107*, 2422.
(26) Eggeling, C.; Volkmer, A.; Seidel, C. A. M. *Chem. Phys. Chem.* **2005**, *6*, 791.
(27) Zondervan, R.; Kulzer, F.; Orlinskii, S. B.; Orrit, M. *J. Phys. Chem. A* **2003**, *107*, 6770.
(28) Zondervan, R.; Kulzer, F.; Kol'chenko, M. A.; Orrit, M. *J. Phys. Chem. A* **2004**, *108*, 1657.
(29) Panzer, O.; Göhde, W.; Fischer, U. C.; Fuchs, H.; Müllen, K. *Adv. Mater.* **1998**, *17*, 1469.
(30) Meneses-Nava, M. A.; Chavez-Cerda, S.; Sanchez-Villicana, V.; Sanchez-Mondragon, J. J.; King, T. A. *Opt. Mater.* **1999**, *12*, 441.
(31) Weston, K.-D.; Carson, P. J.; Metiu, H.; Buratto, S. K. *J. Chem. Phys.* **1998**, *109*, 7474.
(32) Deschenes, L. A.; Vanden Bout, D. A. *Chem. Phys. Lett.* **2002**, *365*, 387.
(33) Hofkens, J.; Maus, M.; Gensch, T.; Vosch, T.; Cotlet, M.; Köhn, F.; Hermann, A.; Müllen, K.; De Schryver, F. C. *J. Am. Chem. Soc.* **2000**, *122*, 9278.
(34) Lam, S. K.; Namdas, E.; Lo, D. *J. Photochem. Photobiol.* **1998**, *118*, 25.
(35) Turro, N. J. *Modern Molecular Photochemistry*; Benjamin/Cummings: Menlo Park, CA, 1978.
(36) Veerman, J. A.; Garcia-Parajo M. F.; Kuipers, L.; Van Hulst, N. F. *Phys. Rev. Lett.* **1999**, *83*, 2155.
(37) Weston, K.-D.; Carson, P. J.; DeAro, J. A.; Buratto, S. K. *Chem. Phys. Lett.* **1999**, *308*, 58.
(38) English, D. S.; Furube, A.; Barbara, P. F. *Chem. Phys. Lett.* **2000**, *324*, 15.
(39) Schweitzer, C.; Mehrdad, Z.; Noll, A.; Grabner, E. W.; Schmidt, R. *J. Phys. Chem. A* **2003**, *107*, 2192.
(40) Wennmalm, S.; Rigler, R. *J. Phys. Chem. B* **1999**, *103*, 2516.
(41) Molski, A. *J. Chem. Phys.* **2001**, *114*, 1142.
(42) Berglund, A. J. *Chem. Phys.* **2004**, *2899*, 2004.
(43) Christ, T.; Kulzer, F.; Weil, T.; Müllen, K.; Basché, Th. **2003**, *372*, 878.
(44) Vosch, T.; Cotlet, M.; Hofkens, J.; Van der Biest, K.; Lor, M.; Weston, K.; Tinnefeld, P.; Sauer, M.; Latterini, L.; Müllen, K.; De Schryver, F. C. *J. Phys. Chem. A* **2003**, *107*, 6920.
(45) Eggeling, C.; Widengren, J.; Rigler R.; Seidel C. A. M. *Anal. Chem.* **1998**, *70*, 2651.
(46) Sadrai, M.; Hadel, L.; Sauers, R. R.; Husain, S.; Krog-Jespersen K.; Westbrook, J. D.; Bird, G. R. *J. Phys. Chem. A* **1992**, *96*, 7988.
(47) Azoulay, J. Ph.D. thesis, University Paris XI, Orsay, France, 2001.
(48) Lor, M.; Thielemans, J.; Viaene, L.; Cotlet, M.; Hofkens, J.; Weil, T.; Hampel, C.; Müllen K.; Verhoeven, J. W., Van der Auweraer, M.; De Schryver, F. C. *J. Am. Chem. Soc.* **2002**, *124*, 9918.
(49) Rettig, W.; Zander, M. *Ber. Bunsen-Ges. Phys. Chem.* **1983**, *87*, 1143.
(50) Maus, M.; Rettig, W.; Bonafoux, D.; Lapouyade, R. *J. Phys. Chem. A* **1999**, *103*, 3388.